Inter-comparison of Elemental and Organic Carbon Mass Measurements from Three North American National Long-term Monitoring Networks at a co-located Site

Tak W. Chan[1,*], Lin Huang[1,*], Kulbir Banwait[2], Wendy Zhang[1], Darrell Ernst[1], Xiaoliang Wang[3], John G. Watson[3], Judith C. Chow[3], Mark Green[3], Claudia I. Czimczik[4], Guaciara M. Santos[4], Sangeeta Sharma[1], Keith Jones[5]

[1] Climate Chemistry Measurements and Research, Climate Research Division, Environment and Climate Change Canada, 4905 Dufferin Street, Toronto, Ontario, Canada, M3H 5T4

[2] Measurements and Analysis Research Section, Air Quality Research Division, Environment and Climate Change Canada, 4905 Dufferin Street, Toronto, Ontario, Canada, M3H 5T4

[3] Division of Atmospheric Sciences, Environmental Analysis Facility, Desert Research Institute, 2215 Raggio Parkway, Reno, NV 89512

[4] Earth System Science, University of California, Irvine, CA 92697-3100, USA

[5] Applied Environmental Prediction Science Pacific & Yukon, Prediction Services Operations West, Prediction Services Directorate, Meteorological Service of Canada, #201-401 Burrard Street, Vancouver, B.C., Canada, V6C 3S5

* Corresponding authors, Email: tak.chan@canada.ca, Phone: (416) 739-4419; lin.huang@canada.ca, Phone: (416) 739-5821

Keywords

Black carbon, thermal evolution, air pollution, carbonaceous aerosol, IMPROVE, CAPMoN, CABM

Abstract

Carbonaceous aerosol is a major contributor to the total aerosol load and being monitored by diverse measurement approaches. Here, ten years (2005-2015) of continuous carbonaceous aerosol measurements collected at the Centre of Atmospheric Research Experiments (CARE) in Egbert, Ontario, Canada on quartz-fiber filters by three independent networks (Interagency Monitoring of PROtected Visual Environments (IMPROVE), Canadian Air and Precipitation Monitoring Network (CAPMoN), and Canadian Aerosol Baseline Measurement (CABM)) were compared. Specifically, the study evaluated how differences in sample collection and analysis affected the concentrations of total carbon (TC), organic carbon (OC), and elemental carbon (EC). Results show that different carbonaceous fractions measured by various networks were consistent and comparable in general among the three networks over the ten years period, even with different sampling systems/frequencies, analytical protocols and artifact corrections. The CAPMoN TC, OC, and EC obtained from the DRI-TOR method were lower than those determined from the IMPROVE_A TOR method by 17%, 14% and 18%, respectively. When using transmittance for charring correction, the corresponding carbonaceous fractions obtained from the Sunset-TOT were lower by as much as 30%, 15%, and 75%, respectively. In comparison, the CABM TC, OC, and EC obtained from a thermal method (ECT9) were higher than the corresponding fractions from IMPROVE_A TOR by 20-30%, 0-15% and 60-80%, respectively. Ambient OC and EC concentrations were found to elevate when ambient temperature exceeded 10 °C. These increased ambient concentrations of OC during summer were possibly attributed to the secondary organic aerosol (SOA) formation and forest fire emissions, while elevated EC concentrations were potentially influenced by forest fire emissions and increased vehicle emissions. Results also show that the pyrolyzed organic carbon (POC) obtained from the EnCan-Total-900 (ECT9) protocol could provide additional information on SOA although more research is still needed.

Introduction

Carbonaceous aerosols, including elemental carbon (EC), which is often referred to as black carbon (BC) and organic carbon (OC), make up a large fraction of the atmospheric fine particulate matter (PM) mass (Heintzenberg, 1989). Atmospheric OC and BC particles that are emitted directly into the atmosphere have both natural (e.g., biomass burning or forest fires) and anthropogenic (e.g., internal combustion engines) sources. A significant amount of the particulate OC is also formed in the atmosphere through oxidation and condensation of volatile organic compounds (e.g., isoprene and terpenes), which are emitted directly from vegetation. BC is a by-product of incomplete combustion of

hydrocarbon fuels, generated mainly from fossil fuel combustion and biomass burning. Atmospheric particles have direct and indirect influences on climate, visibility, air quality, ecosystems, and adverse human health effects (Bond et al., 2013; Japar et al 1986; Lesins et al., 2002; Watson, 2002). Atmospheric BC absorbs solar radiation while OC primarily scatters (Schulz et al., 2006). However, BC and OC co-exist in atmospheric particles and the net radiative forcing of the aerosol particles depends on the particle size, composition, and the mixing state of the particles, while all of these variables also change as aerosol particles age (Fuller et al., 1999; Lesins et al., 2002).

Black carbon is a generic term in the literature and it is often interchanged with other terms such as EC, soot, refractory BC, light absorbing carbon, or equivalent BC (Petzold et al., 2013). Although BC is highly relevant to climate research, there is no universally agreed and clearly defined terminology concerning the metrics of carbonaceous aerosol. The use of different terminology is linked to the different methodologies used to measure different physical or chemical properties of BC. The scientific community generally accepts the definitions that BC particles possess the following properties: (1) strongly absorbing in the visual spectrum with an inverse wavelength (λ) dependence (i.e., λ^{-1}) (Bond and Bergstrom 2006), (2) refractory in nature with a vaporization temperature near 4000 K (Schwarz et al., 2006), (3) insoluble in water and common organic solvents (Fung, 1990), (4) fractal-like aggregates of small carbon spherules (Kittelson, 1998), (5) containing a large fraction of graphite-like sp^2-bonded carbon atoms (Bond et al., 2013; Petzold et al., 2013), and (6) chemically inertness in the atmosphere (Bond et al. 2013). In this article, the recommendation from Petzold et al. (2013) is adopted as the definition of BC whenever the context of climate effects impacted by strong light-absorption carbonaceous substance is mentioned. EC is referred to as the carbon mass determined from the thermal evolution analysis (TEA) or thermal optical analysis (TOA) of carbonaceous materials at the highest temperature set point (e.g., >550 °C) under an oxygenated environment. It is also assumed that ambient EC and BC concentrations time series correlate with each other.

TOA and TEA have been applied in many long-term monitoring networks with various protocols to quantify OC and EC concentrations from aerosol deposits on quartz-fiber filters (Birch and Cary, 1996; Cachier et al., 1989; Cavalli et al., 2010; Chow et al., 1993; Huang et al., 2006; Huntzicker et al., 1982) due to the simplicity in filter sample collection and the analytical procedures. TOA and TEA provide a direct measurement of the carbon mass in the collected PM mass. One of the limitations of TOA and TEA is the need for sufficient sampling time to accumulate enough mass for precise measurements (i.e., ensuring a high signal to noise ratio) which constrains the temporal resolution of such samples. In

addition, EC and OC are defined differently in different protocols and could affect the absolute mass values measured. Generally, OC is quantified under a pure helium (He) atmosphere at a low heating temperature whereas EC is quantified under an oxygen (O_2)/He atmosphere at high temperatures. Estimates of total carbon (TC=OC+EC) derived from different TOA and TEA methods are generally consistent, whereby the differences in OC and EC estimates could vary from 20 to 90%, and often larger differences are found for EC, owing to its smaller contribution to TC (Cavalli et al., 2010; Chow et al., 1993; 2001; 2005; Countess 1990; Watson et al., 2005; Hand et al., 2012).

During thermal analysis, some of the OC chars to form pyrolyzed organic carbon (POC) when heated in the inert He atmosphere, darkening the filter (Chow et al., 2004; Watson et al. 2005). When O_2 is added, POC combusts to EC, resulting in an overestimation of EC of the filter. The formation of POC depends on the nature of the organic materials, the amount of the oxygenated compounds in the collected particles, the rate, duration, and temperature of the heating, and the supply of O_2 in the carrier gas (Cachier et al. 1989; Chan et al., 2010; Han et al. 2007; Yang and Yu, 2002). POC in TOA is estimated by monitoring reflectance and/or transmittance of a 633-650 nm laser beam, which is termed thermal optical reflectance (TOR) or thermal optical transmittance (TOT) method, respectively. When the reflected or transmitted laser signal returns to its initial intensity at the start of the analysis (i.e., at OC/EC split point), it is assumed that artifact POC has left the sample and the remaining carbon belongs to EC. The carbon mass before the split point is defined as OC whereas that after the split point is defined as EC. POC is defined as the mass determined between the time when O_2 is introduced and the OC/EC split point. Different from TOA, the TEA used in this study applies a different approach for POC determination (see below).

Quartz-fiber filters adsorb organic vapors (Chow et al., 2009; Turpin et al., 1994; Viana et al., 2006; Watson et al., 2010), resulting in non-PM contributions to OC and charring enhancement within the filter. These vapors are adsorbed passively when the filter is exposed to air and more so as air is drawn through the filter during PM sampling. Sampling at low filter face velocities for long period of time could lead to more adsorption (McDow and Huntzicker, 1990), while using high filter face velocities for longer sample durations may result in evaporation of semi-volatile compounds as negative artifact (Khalek, 2008; Sutter et al., 2010; Yang et al., 2011). The positive OC artifact from adsorption usually exceeds the negative evaporation artifact, especially at low temperatures, resulting in OC overestimation (Watson et al., 2009; WMO, 2016). This can be corrected by subtracting the OC

concentration from field blanks or backup filters located downstream of a Teflon-membrane or quartz-fiber filter (Chow et al., 2010; Watson et al., 2005; 2010).

Previous studies further suggested that TOT could over-estimate the POC mass more than TOR, resulting in higher POC (and lower EC) because of the charring of the adsorbed organic vapors within the filter (Chow et al 2004; Countess 1990). Since only a portion (0.5-1.5 cm^2) of the filter is analyzed, inhomogeneous PM deposits add to measurement uncertainty when OC and EC are normalized to the entire filter deposit area. Deposits that are light or too dark can cause unstable laser signals that affect the OC/EC split (Watson et al., 2005).

The short lifetime of atmospheric aerosols (in days to weeks) and the different chemical and microphysical processing that occur in the atmosphere result in high spatial and temporal variations of aerosol properties. To facilitate the determination of the trends in emission changes and evaluation of the effectiveness of emission mitigation policies (Chen et al. 2012), long-term consistent atmospheric measurements are required, including aerosol carbon fractions. The emission sources of OC and EC at a regional and global scales are often constrained through the use of atmospheric transport models in conjunction of long-term OC and EC measurements (Collaud Coen et al., 2013; Huang et al., 2018). Usually an integration of datasets from different networks is necessary for sufficient spatial coverage. The objective of this study is to conduct an inter-comparison study for evaluating the comparability and consistency of ten years co-located carbonaceous aerosol measurements at Egbert made by three North American networks (Interagency Monitoring of PROtected Visual Environments, Canadian Air and Precipitation Monitoring Network, and Canadian Aerosol Baseline Measurement), all of which use different sampling instruments, frequencies, durations, analytical methods, and artifact corrections. This inter-comparison study is also expected to provide some suggestions/recommendations for improving the compatibility and consistency of long-term measurements.

Sampling and Measurements

Sampling Site

The sampling station is the Center for Atmospheric Research Experiments (CARE) located near Egbert, Ontario (44°12´ N, 79°48´ W, 251 m a.s.l.), Canada. This station is owned and operated by Environment and Climate Change Canada (ECCC), and is located 70 km NNW of the city of Toronto. There are no major local anthropogenic sources within about 10 km of the site. Air that reaches this site from southern Ontario and the northeastern United States typically carries urban or anthropogenic

combustion pollutants that were emitted within last two days (Rupakheti et al. 2005; Chan and Mozurkewich 2007; Chan et al., 2010). Air from the north generally contains biogenic emissions and is often accompanied with the presence of SOA during summer (Chan et al., 2010; Slowik et al., 2010). Table 1 compares the instrument and analytical specifications among the three networks.

The Interagency Monitoring of PROtected Visual Environment Network

The IMPROVE network, established in 1987, includes regional-scale monitoring stations for detecting visibility trends, understanding long-term trends, and evaluating atmospheric processes (Malm 1989; Malm et al., 1994; Yu et al., 2004). IMPROVE operates about 150 sites and provides long-term records of PM_{10} and $PM_{2.5}$ (particles with aerodynamic diameter less than 10 and 2.5 microns, respectively) mass as well as $PM_{2.5}$ composition, including anions (i.e., chloride, nitrate, and sulfate), and carbon (OC and EC). IMPROVE 24-hour samples at Egbert were acquired once every third day from 2005 to 2015. The sampling period was from 08:00 to 08:00 local standard time (LST) except for August 16, 2006 through October 24, 2008 (from 00:00 to 00:00 LST). Module C of the IMPROVE sampler uses a modified air-industrial hygiene laboratory (AIHL) cyclone with a 2.5 µm cut point at a flow rate of 22.8 liters per minute (L/min). PM samples were collected onto a 25 mm diameter quartz-fiber filter (Tissue quartz, Pall Life Sciences, Ann Arbor, MI, USA), which were pre-fired at 900°C for four hours. Once sampled, filters were stored in freezer until they were ready to be analyzed in the DRI laboratory in Reno. All samples were analyzed by the IMPROVE_A thermal/optical reflectance protocol (Figure S1a; Supplementary information) (Chow et al., 2007) as shown in Table S1 (Supplementary information). The IMPROVE data (denoted as IMPROVE_A TOR) were obtained from the website http://vista.cira.colostate.edu/IMPROVE (Malm et al., 1994; IMPROVE, 2017).

The Canadian Air and Precipitation Monitoring Network

CAPMoN was established in 1983 to understand the source impacts of acid rain-related pollutants from long-range transport to the Canadian soil and atmosphere. The network operates 30 regionally representatives sites (as of 2015) across Canada with most located in Ontario and Quebec. Measurements include PM, trace gases, mercury (both in air and precipitation), tropospheric ozone, and multiple inorganic ions in air and precipitation. In addition, a few number of sites include carbon (OC and EC) meausrements (https://www.canada.ca/en/environment-climate-change/services/air-pollution/monitoring-networks-data/canadian-air-precipitation.html).

Twenty-four-hour samples (08:00 to 08:00 LST) were acquired every third day from 2005 to 2015 using the Modified Rupprecht and Patashnick (R&P) Model 2300 $PM_{2.5}$ Speciation Sampler with ChemComb cartridges and $PM_{2.5}$ impactor plates with impactor foam to direct particles onto a 47 mm diameter tissue quartz-fiber filter (Thermo Scientific, Waltham, MA, USA) operated at 10 L/min. Samples were made on the same date when the IMPROVE samples were collected. A second parallel cartridge is configured with a 47 mm front Teflon-membrane filter and a quartz-fiber backup filter to estimate vapor adsorption artifact. All quartz-fiber filters were pre-fired at either 800°C or 900°C for over two hours and cooled at 105°C overnight and stored in freezer (-15 °C) before being used for sampling. All sampled filters were shipped cold and stored in freezer until they are ready to be analyzed in the CAPMoN laboratory in Toronto.

Carbon was determined using the Sunset laboratory-based carbon analyzer (Sunset Laboratory Inc., OR, USA; http://www.sunlab.com/) following the IMPROVE-TOT protocol from 2005 to 2007 (denoted as Sunset-TOT), then by DRI Model 2001 Thermal/Optical Carbon Analyzer following the IMPROVE-TOR protocol (denoted as DRI-TOR) from 2008 to 2015 (Chow et al., 1993). As shown in Table S1, the temperature settings for IMPROVE protocol (i.e., DRI-TOR) for CAPMoN samples are lower than those of IMPROVE_A TOR protocol for IMPROVE samples by 20°C to 40°C (Figure S1b). Overall, Chow et al. (2007) found that the small difference in the temperature-ramp between these protocols results in correlated but different OC, EC, and TC mass.

The Canadian Aerosol Baseline Measurement Network

The Climate Chemistry Measurements and Research (CCMR) Section in the Climate Research Division of ECCC has operated the Canadian Aerosol Baseline Measurement (CABM) network since 2005 to acquire data relevant to climate change (https://www.canada.ca/en/environment-climate-change/services/climate-change/science-research-data/greenhouse-gases-aerosols-monitoring/canadian-aerosol-baseline-measurement-program.html). The CABM network includes 6 sites (as of 2016) for aerosol chemical, physical, and optical measurements that cover ecosystems at coastal, interior urban/rural areas, boreal forests, and the Arctic. Measurements are intended to elucidate influences from various emission sources on regional background air, including biogenic emissions, biomass burning as well as anthropogenic contributions from industrial/urban areas.

The CABM filter pack system uses a $PM_{2.5}$ stainless steel cyclone (URG-2000-30EHS) operated at 16.7 L/min for sampling from 2006 to 2015 with an operator manually changing the 47 mm quartz-fiber

filter on a weekly basis. All quartz-fiber filters were pre-fired at 900°C overnight prior being sampled. Once sampled, filters were shipped cold and then stored in freezer until they were ready to be analyzed in the CCMR laboratory in Toronto. A TEA method, EnCan-Total-900 (ECT9), developed by Huang et al. (2006) and refined later (Chan et al., 2010), was used to analyze the OC, POC, and EC on the quartz-fiber filters using a Sunset laboratory-based carbon analyzer. The ECT9 protocol was developed to permit stable carbon isotope (^{13}C) analysis of the OC and EC masses without causing isotope fractionation, as it was demonstrated by Huang et al. (2006). This method first heats the filter at 550°C and 870°C for 600 s each in the He atmosphere to determine OC and POC (including carbonate carbon; CC), respectively, and then combusts the sample at 900°C under 2% O_2 and 98% He atmosphere for 420 s to determine EC (Figure S1c and Table S1). The ECT9 POC definition (released as CO_2 at 870 °C) includes the charred OC, and some calcium carbonate ($CaCO_3$) that decomposes at 830°C, as well as any refractory OC that is not combusted at 550°C. Chan et al. (2010) found that POC determined by ECT9 was proportional to the oxygenated compounds (e.g., aged aerosol from atmospheric photochemical reaction) and possibly humic-like materials. Consistent with the IMPROVE_A TOR protocol (Chow et al., 2007), OC is defined as the sum of OC and POC, as CC is usually negligible in $PM_{2.5}$.

CABM sites are also equipped with Particle Soot Absorption Photometer (PSAP; Radiance Research, Seattle, WA, USA) that continuously monitor aerosol light absorption at 1 minute time resolution, as changes in the amount of light transmitted through a quartz-fiber filter. Assuming the mass absorption coefficient (MAC) for aerosol is constant at Egbert, the one minute PSAP absorption measurements are linearly proportional to the BC or EC concentrations. In this study, five years of PSAP data (2010-2015) collected at Egbert was used to assess the impact of different sampling duration on the derived monthly averages EC values.

Differences in Sampling and Analysis among Networks

Depending on the sharpness (i.e., slope) of the inlet sampling effectiveness curve (Watson et al., 1983), different size-selective inlets may introduce measurement uncertainties. CAPMoN uses impactors whereas CABM and IMPROVE use cyclones. Impactor may have larger pressure drops across the inlet that might enhance semi-volatile PM evaporation. Larger solid particles might bounce off when in contact with the impactor and be re-entrained in the $PM_{2.5}$ samples if the impactor is overloaded (Flagan and Seinfeld, 1998; Hinds, 1999). Atmospheric mass size distributions typically peak at about 10 µm with a minimum near 2.5 µm, therefore, the difference in mass collected with different impactors or cyclones among the three networks is not expected to be large (Watson and Chow, 2011). Analyzing OC

234 and EC content by TEA or TOA also subject to a number of artifacts, including adsorption of volatile
235 organic compound (VOC) gases by quartz-fiber filter, leading to positive artifact, and evaporation of
236 particles, leading to negative artifact (Malm et al., 2011).

237 The small filter disc (25 mm diameter) and high flow rate (22.8 L/min) in the IMPROVE sampler
238 result in a 5- to 7-fold higher filter face velocity (i.e., 107.7 cm/s) than that for the CAPMoN and CABM
239 samplers (16-20 cm/s). McDow and Huntzicker (1990) assert that higher filter face velocity may reduce
240 sampling artifacts. However, very high face velocity (>100 cm/s) may enhance OC volatilization (Khalek
241 2008).

242 Both IMPROVE and CAPMoN networks correct for vapor adsorption, while CABM network does
243 not. For CAPMoN measurements, the organic artifact derived from each 24-hour backup quartz-filter
244 was subtracted from the corresponding OC measurement. For IMPROVE measurements (up until 2015),
245 monthly median OC value obtained from the backup quartz-filters from 13 sites (not including Egbert)
246 was subtracted from all samples collected in the corresponding month. Monthly averaged OC values
247 were then derived from the 24-hour artifact corrected measurements.

248 Multiple studies show that using the same TOA protocol on both DRI and Sunset carbon
249 analyzers can produce comparable TC concentrations (Chow et al., 2005; Watson et al., 2005).
250 However, large differences in EC are found between the reflectance and transmittance POC correction
251 (Chow et al., 2004; 2005; Watson et al., 2005). Difference in OC and EC definitions among different TOA
252 and TEA protocols introduces measurement uncertainties. Among the TOA methods, how POC is
253 determined from the laser signals at different temperatures in the inert He atmosphere introduce
254 uncertainties. Large uncertainties in laser transmittance were found for lightly- and heavily-loaded
255 samples (Birch and Cary, 1996). For the CABM samples, the POC determined at 870 °C by ECT9
256 represents different OC properties and does not equal the charred OC obtained by Sunset-TOT, DRI-TOR,
257 or IMPROVE_A TOR.

258 Both IMPROVE and CAPMoN data sets are once every third day 24-hour measurements
259 collected on the same date while the CABM data is weekly integrated samples. A comparison between
260 the integrated weekly samples and 24-hour samples have already been done by Yang et al. (2011) and
261 therefore will not be repeated here. Based on two years of Egbert measurements (2005-2007), Yang et
262 al. (2011) suggested that integrated weekly samples might experience reduced vapor adsorption but
263 increased losses of semi-volatile organics leading to lower OC measurements. Weekly EC values were

higher than those from 24-hour samples, which were attributed to the higher analytical uncertainties for the lower loadings on the 24-hr samples (Yang et al., 2011).

Five years (2010-2015) of real-time (1 min average) PSAP particle light absorption measurements (at 567 nm) was used here as a proxy common EC data set to assess the effect of different sample duration on monthly average EC concentrations. First, the 1 min PSAP data was averaged to 24-hour once in every three day samples and integrated weekly samples, respectively, and the comparison of the two data sets are compared in Figure 1a. The results demonstrate that both data sets capture the variations adequately. Monthly averages derived from the two sets of measurements show highly correlated results (r=0.78; Figure 1b) and a slope of 0.96 (Figure 1c). Assuming the variations in light absorption can represent the variations in EC, these results suggest that monthly averaged EC based on integrated weekly sampling is about 4% lower than the monthly averaged EC based on 24 hour sampling.

Results and Discussions

NIST urban dust standard comparison

The National Institute of Standards and Technology (NIST) Urban Dust Standard Reference Material (SRM) 8785 Air Particulate Matter on Filter Media is intended primarily for use to evaluate analytical methods used to characterize the carbon composition of atmospheric fine PM (Cavanagh and Watters, 2005; Klouda et al., 2005). These samples were produced by resuspension of the original SRM 1649a urban dust sample, followed by collection of the fine fraction ($PM_{2.5}$) on quartz-fiber filters (Klouda et al., 2005; May and Trahey, 2001). Past studies on SRM 1649a and SRM 8785 have shown consistent composition and both samples were supplied with certified values for OC and EC (Currie et al., 2002; Klouda et al., 2005). The consistency between the ECT9 and the IMPROVE_A TOR analytical methods was assessed by analyzing NIST SRM 8785 filters. Four SRM 8785 filters with mass loading of 624-2262 μg were analyzed following the ECT9 method by the ECCC laboratory and the IMPROVE_A TOR protocol by the DRI laboratory during 2009-2010.

The values in the SRM 8785 certificate were reported in grams of OC or EC per grams of PM mass, which are average mass ratios based on analysis of a small numbers of randomly selected samples. Figure 2a-c shows that measurements by IMPROVE_A TOR protocol were within uncertainties of the certificate values. Ratios measured with ECT9 were greater, but not significantly different from the certificate values. When fitting the ECT9 measurements to the IMPROVE_A TOR measurements

using a linear regression (Figure 3a-c), good correlations (r=0.9-0.99) were observed with 21-25% higher in values by the ECT9 method than the IMPROVE_A TOR.

The parameter EC/TC, calculated based on the reported certificate values, were compared with the average EC/TC values determined from the inter-comparison study (ICP) by the DRI group (using IMPROVE_A TOR) and the ECCC group (using ECT9) (Figure 2d). These results show that EC/TC reported by both analytical methods were statistically the same as the certificate value.

Finally, the EC/TC value was further verified by analyzing SRM 1649a samples with the ECT9 method. The combusted CO_2 from OC, EC, and TC were analyzed for the isotope ratios (i.e., $^{14}C/^{12}C$) expressed as a fraction of modern carbon (i.e., FM_i is the ratio of $^{14}C/^{12}C$ in the sample i, relative to a modern carbon standard) for individual mass fractions (i.e., FM_{TC}, FM_{OC}, and FM_{EC}). Using isotopic mass balance, the EC/TC ratio can be derived from Eq. [1]:

$$FM_{TC} = FM_{OC} \times \left(1 - \frac{EC}{TC}\right) + FM_{EC} \times \frac{EC}{TC} \qquad [1]$$

The $^{14}C/^{12}C$ ratio were determined by off-line combustion method at the Keck Carbon Cycle accelerator mass spectrometry (KCCAMS) Facility at University of California Irvine. A FM_{TC} value of 0.512 was obtained, which is close to certificate values that range from 0.505 to 0.61 (Currie et al., 2002). Average measured values of FM_{OC} and FM_{EC} for the SRM 1649a via ECT9 were 0.634 (n=3) and 0.349 (n=3), respectively. This yields an EC/TC ratio of 0.425, which is comparable to the ECT9 value of 0.44, and close to the reported certificate value of 0.49 and the IMPROVE_A TOR value of 0.47 (Figure 3d), reconfirming a good separation of OC from EC using the ECT9 method. This analysis also confirms the consistency between the IMPROVE_A TOR and ECT9 methods.

Vapor Adsorption Corrections

Figure 4 shows the monthly averaged carbon concentration time series with and without the artifact correction for CAPMoN samples over the period from 2005 to 2015. Vapor adsorption contributes to a large amount of the measured OC (Figure 4a), but a negligibly amount to EC (Figure 4b) and POC after 2008 (Figure 4c). The median vapor adsorption artifact was 0.79 μg/m^3 from 2008 to 2015 for DRI-TOR, representing about 50.9% of the uncorrected OC, compared to 0.92 μg/m^3 (43.3% of uncorrected OC) using the Sunset-TOT before 2008 (Supplemental Figure S2). Linear least square regressions between corrected and uncorrected carbon in Figure 5 shows a slope of 0.52 for OC and 0.56 for TC with good correlations (r=0.93-0.94). Sunset-TOT measurements acquired prior 2008 are

mostly scattered around the regression line, with higher concentrations. On average, about 48% of the uncorrected OC (0.84 μg/m^3) can be attributed to vapor adsorption. The low filter face velocity (15.5 cm/s) in CAPMoN samples could be one of the contributing factors.

Figure 5c indicates that artifact corrected EC concentrations are 7.8% (0.02 μg/m^3) lower than the uncorrected values. The artifact magnitude is close to the detection limit of 0.022 μg/m^3 (0.197 μg/cm^2) and within analytical uncertainties (Chow et al., 1993). Some Sunset-TOT EC measurements are scattered from the regression line, indicating a more accurate and consistent adsorption correction for DRI-TOR (Figure 5b). Although not expected to impact EC concentration, vapor adsorption directly affects POC correction and thus influences EC mass determination.

Figure 5d shows that 4.3% (0.01 μg/m^3) of POC was caused by vapor adsorption using the DRI-TOR protocol. For Sunset-TOT, however, up to 21.1% (0.17 μg/m^3) of the POC was detected on the backup filter. Note that POC is part of OC and is a charring correction in the DRI-TOR and Sunset-TOT protocols. Results show that filter transmittance is influenced by both surface and within filter charring and EC from different sources have been observed to have different filter penetration depths (Chen et al., 2004; Chow et al., 2004). Based on the available information from this study, an optical correction by reflectance appears to be more appropriate and give more consistent results when POC concentration is relatively large compared to EC (Chen et al., 2004). Regardless, the absolute POC and EC concentrations were much lower than OC and the adsorption correction on TC is mostly attributed to the OC artifact.

Since the IMPROVE aerosol samples were acquired at a higher filter face velocity (107.7 cm/s), it is expected that the magnitude of the vapor adsorption correction would be smaller for the IMPROVE samples. This is supported by the observations from Watson et al. (2009) at six anchor IMPROVE sites (i.e., Mount Rainier National Park, Yosemite National Park, Hance Camp at Grand Canyon National Park, Chiricahua National Monument, Shenandoah National Park, and Okefenokee National Wildlife Refuge), suggesting that vapor adsorption obtained from backup quartz filters represented about 23% of the uncorrected OC values. Filter fibers are saturated over a long sampling interval (Khalek, 2008; Watson et al., 2009), thus, artifacts for the CABM samples are expected to be lower relatively.

Comparison among IMPROVE, CAPMoN, and CABM Measurements

Figure 6 shows the temporal variations of the monthly averaged IMPROVE_A TOR, CAPMoN Sunset-TOT, DRI-TOR, and CABM ECT9 measurements. Also included in the figure are the monthly

averaged temperature and the wind direction and speed (expressed in wind barbs). It is evident that better correlations of TC, EC and OC were found between the protocols that use same POC correction method (DRI-TOR and IMPROVE_A TOR) than between Sunset-TOT (which uses transmittance for POC correction) and IMPROVE_A TOR (Table 2). Especially correlation of EC between Sunset-TOT and IMPROVE_A TOR was poor.

Comparisons of the monthly averaged carbonaceous measurements among different networks are summarized in Figure 7. When fitting the monthly averaged DRI-TOR and Sunset-TOT measurements to IMPROVE_A TOR measurements using a linear regression fit through the origin (i.e., Regression 1) typically yields less than unity slopes (0.64-0.97; Table 2), suggesting that the carbonaceous masses reported by CAPMoN were in general lower than those by IMPROVE. Fitting the measurements allowing an intercept (i.e., Regression 2) typically yields least square slopes close to unity (>0.92) with small intercepts.

The effect of using transmittance or reflectance for POC determination is apparent. The Sunset-TOT POC correction is larger because transmittance is affected by the charred OC within the filter. This is consistent with the larger regression slopes in POC (Regression 1: 1.8) between Sunset-TOT and IMPROVE_A TOR protocol than the slope in POC (1.0) between the DRI-TOR and IMPROVE_A TOR protocol.

The ECT9 versus IMPROVE_A TOR via Regression 1 slopes are equal to or greater than unity, ranging from 1.0 to 1.8 (Table 2). Linear regression with intercept (i.e., Regression 2) yields lower slopes (0.6-1.7) with positive intercepts (0.06-0.18 $\mu g/m^3$), signifying higher TC and EC concentrations for ECT9 samples. Higher intercepts (0.12-0.18 $\mu g/m^3$) for TC, OC, and POC are consistent with ECT9 measurements uncorrected for vapor adsorption. However, the systematically higher TC, OC and EC by 21-25% via ECT9 relative to those via IMPROVE_A TOR in SRM 8785 could not be simply attributed to the uncorrected vapor adsorption.

In specific, ECT9 OC concentrations are 15% higher than the IMPROVE_A TOR measurements (Table 2) with good correlation (r=0.87; Table S2). the ECT9 method yielded 66-83% higher EC than IMPROVE_A TOR, with moderate correlation (r=0.74). Differences in combustion temperatures for OC/EC split determination could contribute to these discrepancies. Heating under an oxidative environment at a constant temperature of 900 °C in the ECT9 protocol could combust more highly refractory carbon than the IMPROVE_A TOR protocol, which only heats progressively from 580 °C to 840

°C. Another minor factor could include inhomogeneous deposition of mass loading on the filter spot. When plotted on different scales, Figure S3 shows that the two EC data sets track well, capturing both long-term trends and seasonal variations.

A slope approaching unity (1.00) was obtained when fitting the ECT9 POC to IMPROVE_A TOR POC through the origin (Figure 7d). Refitting the data allowing an intercept leads to a slope of 0.62 with a y-intercept (0.12; Table 2), comparable in magnitude to the vapor adsorption artifact. The correlation coefficient between ECT9 POC and IMPOVE_A TOR POC is low (r=0.46; Table S3). However, correlation between IMPROVE_A TOR POC and IMPROVE_A TOR OC is much higher (r=0.91), and even to a lesser extent between IMPROVE_A TOR POC and IMPROVE_A TOR EC (r=0.71). In comparison, ECT9 POC has weak correlation with ECT9 OC (r=0.65) and ECT9 EC (r=0.37). These observations show that the POC definition in ECT9 is not dominated by charred OC correction and likely include the characterization of other oxygenated organic materials as observed in Chan et al. (2010). Additional research is needed to verify if ECT9 POC is proportional to SOA formation.

Seasonality in Carbon Concentration and Possible Origination

Figure 6 shows elevated carbon during summer, consistent with the observations from Yang et al. (2011) and Healy et al. (2017). A sigmoid function was applied here to characterize the relationship between ambient carbon concentration and ambient temperature. The Sigmoid function has a characteristic "S" shape and represents an integral of a Gaussian function. Relationships between carbon concentrations and ambient temperatures are illustrated in Figure S5. Apparent increases in OC and TC concentrations are found when ambient temperatures exceed about 10 °C; a phenomenon not as apparent in EC. EC from the week-long CABM samples are more scattered.

The TC, OC, and EC from all measurements are averaged and shown in Figure 8 with the following best-fitted sigmoid functions:

$$TC = 1.053 + \left\{\frac{3.558}{1+exp\left(\frac{23.081-T}{3.760}\right)}\right\} \quad [2]$$

$$OC = 0.780 + \left\{\frac{1.838}{1+exp\left(\frac{20.089-T}{2.978}\right)}\right\} \quad [3]$$

$$EC = 0.239 + \left\{\frac{1.446}{1+exp\left(\frac{34.776-T}{8.404}\right)}\right\} \quad [4]$$

Equations [2]-[4] show that lower limits of the observed TC, OC, and EC concentrations are 1.05, 0.78, and 0.24 μgC/m^3, with the half way of the maximum growth curve occurring at about 23 °C, 20 °C, and 35 °C, respectively. The predicted maximum concentrations for TC, OC, and EC are 4.61, 2.62, and 1.69 μgC/m^3, respectively.

Preliminary analysis based on simple wind roses and Lagrangian particle dispersion transport model (FLEXible PARTicle dispersion model) (Stohl et al., 2005) was conducted (Supporting Materials). Results from the analysis appear to suggest that human activities (e.g., local transportation, residential heating, and industrial activities), biogenic emissions (e.g., monoterpenes) from the boreal forest, SOA formation, biomass burning, and transboundary transport could contribute to the variations of OC and EC at Egbert in a complicated way (Ding et al., 2014; Chan et al., 2010; Leaitch et al., 2011; Passonen et al., 2013; Tunved et al., 2006; Lavoué et al 2000; Healy et al. 2017), which requires additional research to confirm. At Egbert, increasing ambient temperature from 10 °C to 20 °C leads to higher OC concentrations from 0.84 to 1.61 μgC/m^3 (91.7% increase) and EC concentration from 0.31 to 0.45 μgC/m^3 (45.2% increase). The temperature dependency of OC and EC suggests a potential climate feedback mechanism consistent with the observations from Leaitch at al. (2011) and Passonen et al. (2013).

Chan et al. (2010) showed that ECT9 POC possesses a positive relationship with oxygenated organics and aged aerosol particles. The seasonality in ECT9 POC is compared with the average OC and EC seasonality observed at Egbert (Figure 8d). Interestingly, the ECT9 POC concentration does not show a gradual exponential shape of function as for OC and EC. Instead, it shows a small but obvious two-step function when plotted against ambient temperature. The ECT9 POC temperature dependent results (Figure 8d) suggest constant sources of background emissions of possible oxygenated organic compounds that is independent from the measured OC, with additional secondary organic compound (SOA) formation at higher temperatures (e.g., >15 °C). Future study is needed to verify this.

Summary of the Inter-comparison Study

Ten years of OC and EC measurements at Egbert were obtained from three independent networks (IMPROVE, CAPMoN, CABM) and observable differences in carbon concentrations were attributed to different sampling methods, analytical protocols, sampling time, and filter artifact corrections. Vapor adsorption did not affect EC values but contributed 20-50% of the measured OC, depending on the sampling filter face velocity. The higher TC and OC concentration of the CABM

measurements by 20-30% and 15%, respectively, compared to the IMPROVE measurements could be partially due to the absence of vapor adsorption correction. These results are consistent with other inter-comparison study before data adjustments (Hand et al., 2012). The differences in analytical protocol also play a role in causing higher carbon values, supported by the higher TC, OC and EC values from the SRM8785 analysis obtained by the ECT9 method compared to those by IMPROVE_A TOR method. Pyrolyzed OC (POC) from ECT9 is shown to be more than a charring correction and more research is needed to develop its relationship with SOA.

Important observations from the inter-comparison study are: (1) CAPMoN DRI-TOR TC, OC, and EC are 5-17%, 7-16%, and 7-18% lower than the corresponding masses from IMPROVE_A TOR. (2) CAPMoN Sunset-TOT TC, OC, and EC are lower than the IMPROVE_A TOR values by up to 30%, 15%, and 75%. (3) CABM TC, OC and EC by ECT9 are higher than the IMPROVE_A TOR values by 20-30%, 0-15%, and 60-80%, respectively.

Carbon concentrations observed from all three networks exhibited a non-linear positive dependency with ambient temperature, which can be characterized by a sigmoid function. Although further research is needed, preliminary observations suggested that increased anthropogenic activities, urban emissions, SOA formation, forest fire emissions, and long range transport could have an impact on the observed OC and EC at Egbert. The increase in OC concentration with temperature is consistent with the climate feedback mechanisms reported from various studies. The different characteristic temperature dependency of the ECT9 POC suggests the need for future investigation, which could provide additional insights of SOA formation from acquired carbonaceous measurements.

Suggestions Going Forward

Long-term measurements play important roles for detecting the trends in atmospheric compositions, constraining their emission changes, and allow for assessing the effectiveness of emission mitigation policies at regional scales (WMO, 2016; 2003), provided that the measurements are consistent and comparable across different networks. Recognizing the absence of a universally accepted carbonaceous standard, long-term inter-comparison studies become challenging and even more important. Echo the recommendations from the World Meteorological Organization (WMO) guidelines and recommendations for long-term aerosol measurements (WMO, 2016; 2003), this study illustrates the importance of measurement consistency (e.g., sampling method/procedures, analytical instrument/method/protocols and data processing, quality assurance and quality control protocols)

within a network over a long period of time. As indicated in the guidelines, regular inter-comparison of filter samples should be encouraged. These activities include analyzing exchanged common filter samples and co-located filter samples. In addition, there is a need to develop proper reference materials for assessing comparability and consistency, and incorporating the use of such reference as part of the inter-comparison effort.

Nomenclature

AIHL	Air-industrial hygiene laboratory
AMS	Accelerator mass spectrometry
BC	Black carbon
CABM	Canadian Aerosol Baseline Measurement
CAPMoN	Canadian Air and Precipitation Monitoring Network
CARE	Center for Atmospheric Research Experiment
CCMR	Climate Chemistry Measurements and Research
DRI	Desert Research Institute
DRI-TOR	CAPMoN measurements using IMPROVE on DRI analyzer with TOR correction
EC	Elemental carbon
ECCC	Environment and Climate Change Canada
ECT9	EnCan-Total-900 protocol
FID	Flame ionization detector
FLEXPART	FLEXible PARTicle dispersion model
ICP	Inter-comparison study
IMPROVE	Interagency Monitoring PROtected Visual Environments
IMPROVE_A TOR	IMPROVE_A TOR protocol on DRI analyzer
KCCAMS	Keck Carbon Cycle accelerator mass spectrometry
MAC	Mass absorption coefficient
NIST	National Institute of Standard and Technology
OC	Organic carbon
PM	Particulate matter
POC	Pyrolyzed organic carbon
PSAP	Particle Soot Absorption Photometer
SOA	Secondary organic aerosol
SRM	Standard Reference Material
Sunset-TOT	IMPROVE TOT protocol on Sunset analyzer
TC	Total carbon
TEA	Thermal evolution analysis
TOA	Thermal optical analysis
TOR	Thermal optical reflectance
TOT	Thermal optical transmittance
UCI	University of California Irvine
WMO	World Meteorological Organization

Acknowledgements

Authors would like to acknowledge Elton Chan and Douglas Chan of ECCC for providing the FLEXPART model results and providing technical advice. IMPROVE measurements were obtained directly from the IMPROVE web site (http://vista.cira.colostate.edu/IMPROVE/Data/QA_QC/Advisory.htm). IMPROVE is a collaborative association of state, tribal, and federal agencies, and international partners. U.S. Environmental Protection Agency is the primary funding source, with contracting and research support from the National Park Service. IMPROVE carbon analysis was provided by Desert Research Institute. Funding of this study was initiated by Climate Change Technology and Innovation Initiative (CCTI) program, operated through Natural Resources Canada (NRCan), and supported by Clean Air Regulatory Agenda (CARA) initiative and ECCC internal federal funding.

Supplementary Information:

The supplement related to this article, which includes additional details on thermal/optical analysis, the experimental parameters used in different temperature protocols (IMPROVE, IMPROVE_A, ECT9), radiocarbon analysis, vapor adsorption uncertainty, seasonality of carbonaceous measurements, wind rose analysis, and FLEXPART back trajectory analysis at Egbert are available online.

Author Contributions:

TWC and LH wrote the paper, with KB, JW, JCC, CIC, GMS, KJ provide contributions to the article. All authors commented on the manuscript.

Competing interest:

The authors declare that they have no conflict of interest.

References:

Beverly, R.K., Beaumont, W., Tauz, D., Ormsby, K.M., von Reden, K.F., Santos, G.M. and Southon, J.R.: The Keck Carbon Cycle AMS Laboratory, University of California, Irvine: Status report, Radiocarbon 52, 301-309, 2010.

Birch, M. E. and Cary, R. A.: Elemental carbon-based method for monitoring occupational exposures to particulate diesel exhaust, Aerosol Sci. Technol., 25, 221-241, 1996.

Bond, T. C. and Bergstrom, R. W.: Light absorption by carbonaceous particles: An investigative review, Aerosol Sci. Technol., 40, 27-67, 2006.

Bond, T. C., Doherty, S. J., Fahey, D. W., Forster, P. M., Berntsen, T., DeAngelo, B. J., Flanner, M. G., Ghan, S., Karcher, B., Koch, D., Kinne, S., Kondo, Y., Quinn, P. K., Sarofim, M. C., Schultz, M. G., Schulz, M., Venkataraman, C., Zhang, H., Zhang, S., Bellouin, N., Guttikunda, S. K., Hopke, P. K., Jacobson, M. Z., Kaiser, J. W., Klimont, Z., Lohmann, U., Schwarz, J. P., Shindell, D., Storelvmo, T., Warren, S. G., and Zender, C. S.: Bounding the role of black carbon in the climate system: A scientific assessment, J. Geophys. Res. Atmos., 118, 5380-5552, 2013.

Cachier, H., Bremond, M. P., and Buat-Ménard, P.: Thermal separation of soot carbon, Aerosol Sci. Technol., 10, 358-364, 1989.

Cavalli, F., Viana, M., Yttri, K. E., Genberg, J., and Putaud, J. P.: Toward a standardized thermal-optical protocol for measuring atmospheric organic and elemental carbon: The EUSAAR protocol, Atmos. Meas. Tech., 3, 79-89, 2010.

Cavanagh, R. R. and Watters, Jr., R. L.: National Institute of Standards and Technology: Report of Investigation Reference Material 8785: Air particulate matter on filter media (A fine fraction of SRM 1649a urban dust on quartz-fiber filter), 2005.

Chan, T. W. and Mozurkewich, M.: Application of absolute principal component analysis to size distribution data: identification of particle origins, Atmos. Chem. Phys, 7, 887-897, 2007.

Chan, T. W., Huang, L., Leaitch, W. R., Sharma, S., Brook, J. R., Slowik, J. G., Abbatt, J. P. D., Brickell, P. C., Liggio, J., Li, S. M., and Moosmüller, H.: Observations of OM/OC and specific attenuation coefficients (SAC) in ambient fine PM at a rural site in central Ontario, Canada, Atmos. Chem. Phys, 10, 2393-2411, 2010.

Chen, L.-W. A., Chow, J. C., Watson, J. G., Moosmüller, H., and Arnott, W. P.: Modeling reflectance and transmittance of quartz-fiber filter samples containing elemental carbon particles: Implications for thermal/optical analysis, J. Aerosol Sci., 35, 765-780, 2004.

Chen, L.-W. A., Chow, J. C., Watson, J. G., and Schichtel, B. A.: Consistency of long-term elemental carbon trends from thermal and optical measurements in the IMPROVE network, Atmos. Meas. Tech., 5, 2329-2338, 2012.

Chow, J. C., Watson, J. G., Pritchett, L. C., Pierson, W. R., Frazier, C. A., and Purcell, R. G.: The DRI Thermal/Optical Reflectance carbon analysis system: Description, evaluation and applications in U.S. air quality studies, Atmos. Environ., 27A, 1185-1201, 1993.

Chow, J. C., Watson, J. G., Crow, D., Lowenthal, D. H., and Merrifield, T. M.: Comparison of IMPROVE and NIOSH carbon measurements, Aerosol Sci. Technol., 34, 23-34, 2001.

Chow, J. C., Watson, J. G., Chen, L.-W. A., Arnott, W. P., Moosmüller, H., and Fung, K. K.: Equivalence of elemental carbon by Thermal/Optical Reflectance and Transmittance with different temperature protocols, Environ. Sci. Technol., 38, 4414-4422, 2004.

Chow, J. C., Watson, J. G., Louie, P. K. K., Chen, L.-W. A., and Sin, D.: Comparison of $PM_{2.5}$ carbon measurement methods in Hong Kong, China, Environ. Poll, 137, 334-344, 2005.

Chow, J. C., Watson, J. G., Chen, L.-W. A., Chang, M.-C. O., Robinson, N. F., Trimble, D. L., and Kohl, S. D.: The IMPROVE_A temperature protocol for thermal/optical carbon analysis: Maintaining consistency with a long-term database, J. Air Waste Manage. Assoc., 57, 1014-1023, 2007.

578 Chow, J. C., Watson, J. G., Lowenthal, D. H., and Chen, L.-W. A.: Climate change - Characterization of
579 black carbon and organic carbon air pollution emissions and evaluation of measurement methods Phase
580 II: Characterization of black carbon and organic carbon source emissions, Desert Research Institute,
581 Reno, NVDRI 04-307, 2009.

582 Chow, J. C., Bachmann, J. D., Kinsman, J. D., Legge, A. H., Watson, J. G., Hidy, G. M., and Pennell, W. R.:
583 Multipollutant air quality management: Critical review discussion, J. Air Waste Manage. Assoc., 60,
584 1151-1164, 2010.

585 Collaud-Coen, M. C., Andrews, E., Asmi, A., Baltensperger, U., Bukowiecki, N., Day, D., Fiebig, M.,
586 Fjaeraa, A. M., Flentje, H., Hyvarinen, A., Jefferson, A., Jennings, S. G., Kouvarakis, G., Lihavainen, H.,
587 Myhre, C. L., Malm, W. C., Mihapopoulos, N., Molenar, J. V., O'Dowd, C., Ogren, J. A., Schichtel, B. A.,
588 Sheridan, P., Virkkula, A., Weingartner, E., Weller, R., and Laj, P.: Aerosol decadal trends - Part 1: In-situ
589 optical measurements at GAW and IMPROVE stations, Atmos. Chem. Phys, 13, 869-894, 2013.

590 Countess, R. J.: Interlaboratory analyses of carbonaceous aerosol samples, Aerosol Sci. Technol., 12, 114-
591 121, 1990.

592 Currie, L. A., Benner, B. A., Jr., Cachier, H., Cary, R., Chow, J. C., Druffel, E. R. M., Eglinton, T. I.,
593 Gustafsson, Ö., Hartmann, P. C., Hedges, J. I., Kessler, J. D., Kirchstetter, T. W., Klinedinst, D. B., Klouda,
594 G. A., Marolf, J. V., Masiello, C. A., Novakov, T., Pearson, A., Prentice, K. M., Puxbaum, H., Quinn, J. G.,
595 Reddy, C. M., Schmid, H., Slater, J. F., Watson, J. G., and Wise, S. A.: A critical evaluation of
596 interlaboratory data on total, elemental, and isotopic carbon in the carbonaceous particle reference
597 material, NIST SRM 1649a, Journal of Research of the National Institute of Standards and Technology,
598 107, 279-298, 2002.

599 Ding, L., Chan, T. W., Ke, F. and Wang, D. K. W.: Characterization of chemical composition and
600 concentration of fine particulate matter during a transit strike in Ottawa, Canada, Atmos. Environ., 89,
601 433-442, 2014.

602 Flagan, R. C. and Seinfeld, J. H.: Fundamentals of Air Pollution Engineering, Prentice Hall, Englewood
603 Cliffs, NJ, 1988.

604 Fuller, K. A., Malm, W. C., and Kreidenweis, S. M.: Effects of mixing on extinction by carbonaceous
605 particles, Journal of Geophysical Research, 104, 15941-15954, 1999.

606 Fung, K. K.: Particulate carbon speciation by MnO2 oxidation, Aerosol Sci. Technol., 12, 122-127, 1990.

607 Han, Y. M., Cao, J. J., An, Z., Chow, J. C., Watson, J. G., Jin, Z. D., Fung, K. K., and Liu, S.: Evaluation of the
608 thermal/optical reflectance method for quantification of elemental carbon in sediments, Chemosphere,
609 69, 526-533, 2007.

610 Hand, J.L., Schichtel, B.A., Pitchford, M., Malm, W.C., and Frank, N.H. (2012): Seasonal composition of
611 remote and urban fine particulate matter in the United States, Journal of Geophysical Research, 117,
612 D05209, doi:10.1029/2011JD017122..

613 Healy, R. M., Sofowote, U., Su, Y., Debosz, J., Noble, M., Jeong, C. H., Wang, J. M., Hilker, N., Evans, G. J.,
614 Doerksen, G., Jones, K., and Munoz, A.: Ambient measurements and source apportionment of fossil fuel
615 and biomass burning black carbon in Ontario, Atmos. Environ., 161, 34-47, 2017.

616 Heintzenberg, J. (1989). Fine particles in the global troposphere: A review, Tellus, 41, 149-160.

Hinds, W. C.: Straight-line acceleration and curvilinear particle motion. In: Aerosol Technology. Properties, Behavior, and Measurement of airborne Particles, 2nd Ed., John Wiley & Sons, Inc., New York, 1999.

Huang, L., Brook, J. R., Zhang, W., Li, S. M., Graham, L., Ernst, D., Chivulescu, A., and Lu, G.: Stable isotope measurements of carbon fractions (OC/EC) in airborne particulate: A new dimension for source characterization and apportionment, Atmos. Environ., 40, 2690-2705, 2006.

Huang, L.: The issue of harmonizing the methodologies for emission inventories of GHGs with those of SLCFs (in terms of measurement perspective), IPCC Expert Meeting on Short Lived Climate Forcers, Geneva, May 28-31, 2019, https://www.ipcc-nggip.iges.or.jp/public/mtdocs/1805_Geneva.html

Huntzicker, J. J., Johnson, R. L., Shah, J. J., and Cary, R. A.: Analysis of organic and elemental carbon in ambient aerosols by a thermal-optical method. In: Particulate Carbon: Atmospheric Life Cycle, Wolff, G. T. and Klimisch, R. L. (Eds.), Plenum Press, New York, NY, 1982.

IMPROVE: Interagency Monitoring of Protected Visual Environments, National Park Service, Ft. Collins, CO, 2017.

Japar, S. M., Brachaczek, W. W., Gorse, R. A., Jr., Norbeck, J. H., and Pierson, W. R.: The contribution of elemental carbon to the optical properties of rural atmospheric aerosols, Atmos. Environ., 20, 1281-1289, 1986.

Khalek, I. A.: 2007 diesel particulate measurement research, Coordinating Research Council, Alpharetta, GA, 2008.

Kittelson, D. B.: Engines and nanoparticles: A review, J. Aerosol Sci., 29, 575-588, 1998.

Klouda, G. A., Filliben, J. J., Parish, H. J., Chow, J. C., Watson, J. G., and Cary, R. A.: Reference material 8785: Air particulate matter on filter media, Aerosol Sci. Technol., 39, 173-183, 2005.

Lavoué, D., Liousse, C., Cachier, H., Stocks, B. J., and Goldammer, J. G.: Modeling of carbonaceous particles emitted by boreal and temperate wildfires at northern latitudes, J. Geophys. Res. Atmos., 105, 26871-26890, 2000.

Leaitch, W. R., MacDonald, A. M., Brickell, P. C., Liggio, J., Sjostedt, S. J., Vlasenko, A., Bottenheim, J. W., Huang, L., Li, S. M., Liu, P. S. K., Toom-Sauntry, D., Hayden, K. A., Sharma, S., Shantz, N. C., Wiebe, H. A., Zhang, W., Abbatt, J. P. D., Slowik, J. G., Chang, R. Y. W., Russell, L. M., Schwartz, R. E., Takahama, S., Jayne, J. T., Ng, N. L.: Temperature response of the submicron organic aerosol from temperate forests, Atmos. Environ., 45, 6696-6704, 2011.

Lesins, G., Chylek, P., and Lohmann, U.: A study of internal and external mixing scenarios and its effect on aerosol optical properties and direct radiative forcing, J. Geophys. Res., 107, 4904, 10.1029/2001JD000973, 2002.

Malm, W. C.: Atmospheric haze: Its sources and effects on visibility in rural areas of the continental United States, Env. Mon. Ass., 12, 203-225, 1989.

Malm, W. C., Sisler, J. F., Huffman, D., Eldred, R.A., and Cahill, T. A.: Spatial and seasonal trends in particle concentration and optical extinction in the United States, J. Geophys. Res., 99, 1347-1370, 1994.

Malm, W.C., Schichtel, B.A., and Pitchford, M.L.: Uncertainties in $PM_{2.5}$ gravimetric and speciation measurements and what we can learn from them, J. Air & Waste Manage. Assoc., 61, 1131-1149, 2011.

May, W. E. and Trahey, N. M.: National Institute of Standards and Technology: Certificate of Analysis Standard Reference Material 1649a: Urban dust, 2001.

McDow, S. R. and Huntzicker, J. J.: Vapor adsorption artifact in the sampling of organic aerosol: Face velocity effects, Atmos. Environ., 24A, 2563-2571, 1990.

Paasonen, P., Asmi, A., Petäjä, T., Kajos, M. K., Äijälä, M., Junninen, H., Holst, T., Abbatt, J. P. D., Arneth, A., Birmili, W., van der Gon, H. D., Hamed, A., Hoffer, A., Laakso, L., Laaksonen, A., Leaitch, W. R., Plass-Dülmer, C., Pryor, S. C., Räisänen, P., Swietlicki, E., Wiedensohler, A., Worsnop, D. R., Kerminen, V. M., and Kulmala, M.: Warming-induced increase in aerosol number concentration likely to moderate climate change, Nature Geoscience, 6, 438-442, 2013.

Petzold, A., Ogren, J. A., Fiebig, M., Laj, P., Li, S. M., Baltensperger, U., Holzer-Popp, T., Kinne, S., Pappalardo, G., Sugimoto, N., Wehrli, C., Wiedensohler, A., and Zhang, X. Y.: Recommendations for reporting "black carbon" measurements, Atmos. Chem. Phys, 13, 8365-8379, 2013.

Rupakheti, M., Leaitch, W. R., Lohmann, U., Hayden, K., Brickell, P., Lu, G., Li, S. M., Toom-Sauntry, D., Bottenheim, J. W., Brook, J. R., Vet, R., Jayne, J. T., and Worsnop, D. R.: An intensive study of the size and composition of submicron atmospheric aerosols at a rural site in Ontario, Canada, Aerosol Sci. Technol., 39, 722-736, 2005.

Santos, G.M., Moore, R., Southon, J., Griffin, S., Hinger, E., Zhang, D.: AMS 14C preparation at the KCCAMS/UCI Facility: Status report and performance of small samples. Radiocarbon, 49, 255-269, 2007.

Schulz, M., Textor, C., Kinne, S., Balkanski, Y., Bauer, S., Berntsen, T., Berglen, T., Boucher, O., Dentener, F., Guibert, S., Isaksen, I. S. A., Iversen, T., Koch, D., Kirkevag, A., Liu, X., Montanaro, V., Myhre, G., Penner, J. E., Pitari, G., Reddy, S., Seland, O., Stier, P., and Takemura, T.: Radiatives forcing by aerosols as derived from the AeroCom present-day and pre-industrial simulations, Atmos. Chem. Phys, 6, 5225-5246, 2006.

Schwarz, J. P., Gao, R. S., Fahey, D. W., Thomson, D. S., Watts, L. A., Wilson, J. C., Reeves, J. M., Darbeheshti, M., Baumgardner, D. G., Kok, G. L., Chung, S. H., Schulz, M., Hendricks, J., Lauer, A., Kärcher, B., Slowik, J. G., Rosenlof, K. H., Thompson, T. L., Langford, A. O., Loewenstein, M., and Aikin, K.C.: Single-particle measurements of midlatitude black carbon and light-scattering aerosols from the boundary layer to the lower stratosphere, J. Geophys. Res., 111, D16207, doi:10.1029/2006JD007076, 2006.

Slowik, J. G., Stroud, C., Bottenheim, J. W., Brickell, P. C., Chang, R. Y. W., Liggio, J., Makar, P. A., Martin, R. V., Moran, M. D., Shantz, N. C., Sjostedt, S. J., van Donkelaar, A., Vlasenko, A., Wiebe, H. A., Xia, A. G., Zhang, J., Leaitch, W. R., and Abbatt, J. P. D.: Characterization of a large biogenic secondary organic aerosol event from eastern Canadian forests, Atmos. Chem. Phys, 10, 2825-2845, 2010.

Stohl, A., Forster, C., Frank, A., Seibert, P., and Wotawa, G.: Technical note: The Lagrangian particle dispersion model FLEXPART version 6.2, Atmos. Chem. Phys, 5, 2461-2474, 2005.

Sutter, B., Bemer, D., Appert-Collin, J. C., Thomas, D., and Midoux, N.: Evaporation of liquid semi-volatile aerosols collected on fibrous filters, Aerosol Sci. Technol., 44, 395-404, 2010.

693 Tunved, P., Hansson, H. C., Kerminen, V. M., Strom, J., Dal Maso, M., Lihavainen, H., Viisanen, Y., Aalto,
694 P. P., Komppula, M., and Kulmala, M.: High natural aerosol loading over boreal forests, Science, 312,
695 261-263, 2006.

696 Turpin, B. J., Huntzicker, J. J., and Hering, S. V.: Investigation of organic aerosol sampling artifacts in the
697 Los Angeles Basin, Atmos. Environ., 28, 3061-3071, 1994.

698 Viana, M., Chi, X., Maenhaut, W., Cafmeyer, J., Querol, X., Alastuey, A., Mikuska, P., and Vecera, Z.:
699 Influence of sampling artefacts on measured PM, OC, and EC levels in carbonaceous aerosols in an urban
700 area, Aerosol Sci. Technol., 40, 107-117, 2006.

701 Watson, J. G., Chow, J. C., Shah, J. J., and Pace, T. G.: The effect of sampling inlets on the PM_{10} and PM_{15}
702 to TSP concentration ratios, J. Air Pollut. Control Assoc., 33, 114-119, 1983.

703 Watson, J. G.: Critical review: Visibility: Science and regulation, J. Air Waste Manage. Assoc., 52, 628-
704 713, 2002.

705 Watson, J. G., Chow, J. C., and Chen, L.-W. A.: Summary of organic and elemental carbon/black carbon
706 analysis methods and intercomparisons, Aerosol Air Qual. Res., 5, 65-102, 2005.

707 Watson, J. G., Chow, J. C., Chen, L. W. A., and Frank, N. H.: Methods to assess carbonaceous aerosol
708 sampling artifacts for IMPROVE and other long-term networks, J. Air & Waste Manage. Assoc., 59, 898-
709 911, 2009.

710 Watson, J. G., Chow, J. C., Chen, L.-W. A., and Wang, X. L.: Measurement system evaluation for fugitive
711 dust emissions detection and quantification, Desert Research Institute, Reno, NV, 2010.

712 Watson, J. G., and Chow, J. C.: Ambient aerosol sampling in: Aerosol Measurement: Principles,
713 techniques and applications, Third Edition, edited by Kulkarni, P., Baron, P.A., and Willeke, K., pp. 591-
714 614, Hoboken, NJ, USA: Wiley, 2011.

715 WMO/GAW aerosol measurement procedure: Guidelines and recommendations, WMO TD No. 1178,
716 2003.

717 WMO/GAW aerosol measurement procedures: Guidelines and recommendations, 2nd ed. , WMO-No.
718 1177, 2016.

719 Yang, F., Huang, L., Sharma, S., Brook, J. R., Zhang, W., Li, S. M., and Tan, J. H.: Two-year observations of
720 fine carbonaceous particles in variable sampling intervals, Atmos. Environ., 45, 2418-2426, 2011.

721 Yang, H. and Yu, J. Z.: Uncertainties in charring correction in the analysis of elemental and organic
722 carbon in atmospheric particles by thermal/optical methods, Environ. Sci. Technol., 36, 5199-5204,
723 2002.

724 Yu, S. C., Dennis, R. L., Bhave, P. V., and Eder, B. K.: Primary and secondary organic aerosols over the
725 United States: Estimates on the basis of observed organic carbon (OC) and elemental carbon (EC), and
726 air quality modeled primary OC/EC ratios, Atmos. Environ., 38, 5257-5268, 2004.

727 **Table 1** Specifications for the filter sampling systems and analytical instruments/methods used by the three networks.

	IMPROVE	CAPMoN		CABM
Data coverage period	2005-2015	2005-2007	2008-2015	2005-2015
Analytical instrument	DRI	Sunset	DRI	Sunset
Thermal/optical protocol	IMPROVE_A	IMPROVE	IMPROVE	ECT9
Pyrolyzed organic carbon detection	Reflect.	Transmit.	Reflect. & Transmit.	Retention time
Particle size selection method	Cyclone	Impactor plates	Impactor plates	Cyclone
Particle size cut off diameter (nm)	2.5	2.5	2.5	2.5
Sampling flow rate (L/min)	22.8	10.0	10.0	16.7
Filter media model	2500QAT-UP	2500QAT-UP	2500QAT-UP	2500QAT-UP
Quartz filter diameter (mm)	25	47	47	47
Filter deposition exposure area (cm^2)	3.53	10.75	10.75	13.85
Filter face velocity (cm/s)	107.65	15.50	15.50	20.09
Sampling frequency	Daily every 3 days	Daily every 3 days	Daily every 3 days	Integrated weekly
Daily sampled air volume (L/day)	31680	14400	14400	24048
Air volume per sample (m^3)	31.68	14.4	14.4	168.3
Positive artifact correction	Yes	Yes	Yes	No
Filter blank correction	Yes	No	No	Yes
Number of 24-h sample	1228	254	907	-
Number of weekly sample	-	-	-	476
Number of monthly averaged sample	124	28	93	117

728

729

730 **Table 2** Regression results (slope, correlation coefficient, and total number of points) obtained when fitting various CABM (ECT9) and CAPMoN
731 (Sunset-TOT & DRI-TOR) carbonaceous mass concentration time series against IMPROVE (IMPROVE_A TOR) measurements. IMPROVE_A TOR
732 and ECT9 measurements cover the period from 2005 to 2015. Sunset-TOT and DRI-TOR measurements cover the periods for 2005-2008 and
733 2008-2015, respectively. Regression 1 indicates the best-fitted slope through the origin. Regression 2 is the best-fitted slope with intercept (in
734 brackets).

	Regression 1	Regression 2	R	N
Sunset-TOT TC vs IMPROVE_A TOR TC	0.888±0.033	0.713±0.112 (0.301±0.186)	0.78	28
Sunset-TOT OC vs IMPROVE_A TOR OC	0.967±0.041	0.873±0.135 (0.125±0.170)	0.79	28
Sunset-TOT EC vs IMPROVE_A TOR EC	0.639±0.042	0.233±0.130 (0.171±0.053)	0.33	28
Sunset-TOT POC vs IMPROVE_A TOR POC	1.769±0.091	1.776±0.351 (-0.003±0.127)	0.70	28
DRI-TOR TC vs IMPROVE_A TOR TC	0.832±0.015	0.946±0.044 (-0.164±0.059)	0.91	93
DRI-TOR OC vs IMPROVE_A TOR OC	0.835±0.017	0.934±0.046 (-0.116±0.050)	0.90	93
DRI-TOR EC vs IMPROVE_A TOR EC	0.818±0.019	0.929±0.072 (-0.032±0.020)	0.81	93
DRI-TOR POC vs IMPROVE_A TOR POC	0.986±0.028	1.230±0.080 (-0.073±0.023)	0.85	93
ECT9 TC vs IMPROVE_A TOR TC	1.304±0.022	1.197±0.065 (0.164±0.093)	0.88	107
ECT9 OC vs IMPROVE_A TOR OC	1.149±0.021	1.004±0.056 (0.179±0.064)	0.87	107
ECT9 EC vs IMPROVE_A TOR EC	1.834±0.046	1.661±0.149 (0.056±0.046)	0.74	107
ECT9 POC vs IMPROVE_A TOR POC	0.998±0.031	0.615±0.082 (0.124±0.025)	0.59	107

735

736

Figure 1 (a) Real-time Particle Soot Absorption Photometer (PSAP) measurements averaged to match the corresponding sampling frequencies used in different networks. (b) Monthly PSAP measurements derived from (a). (c) Comparison of the different sets of measurements from (b) with the 1:1 line shown in red.

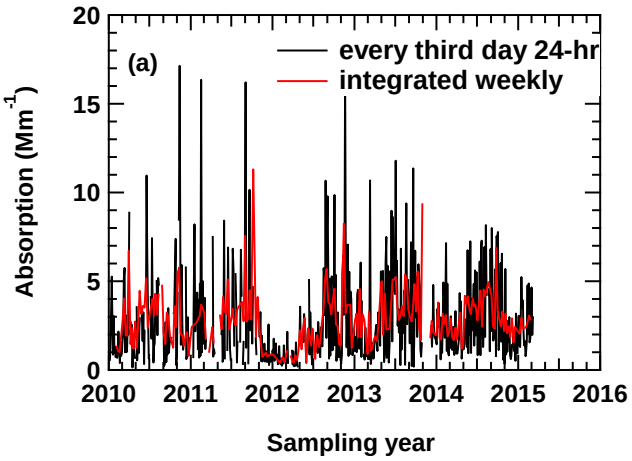

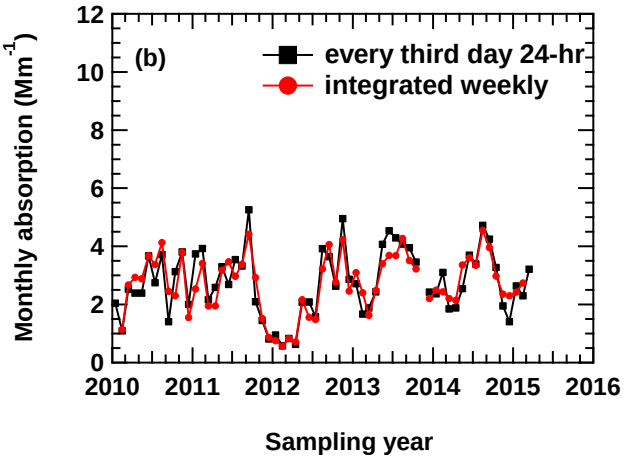

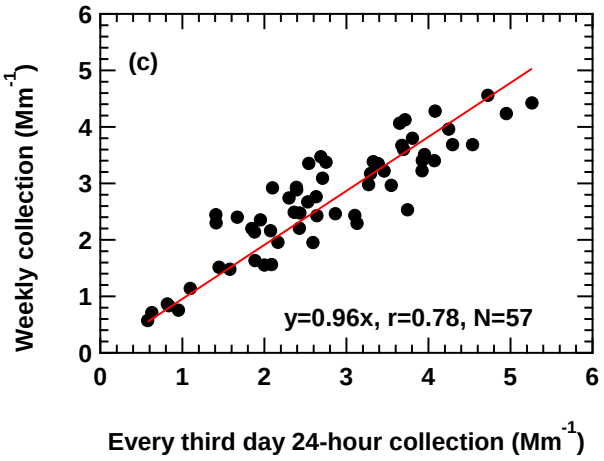

Figure 2 Comparison of the TC, OC, and EC measurements of the NIST SRM samples reported by the ECCC and DRI groups during the inter-comparison study (ICP) conducted between 2009 and 2010. "Reported" represent the published value in the NIST SRM certificate (Cavanagh and Watters, 2005). Error bars represent uncertainties covering 95% confidence interval. In (d), the ECT9 value (in green) represents the calculated EC/TC ratio determined based on stable carbon isotope measurement obtained from the SRM 1649a sample (Currie et al., 2002).

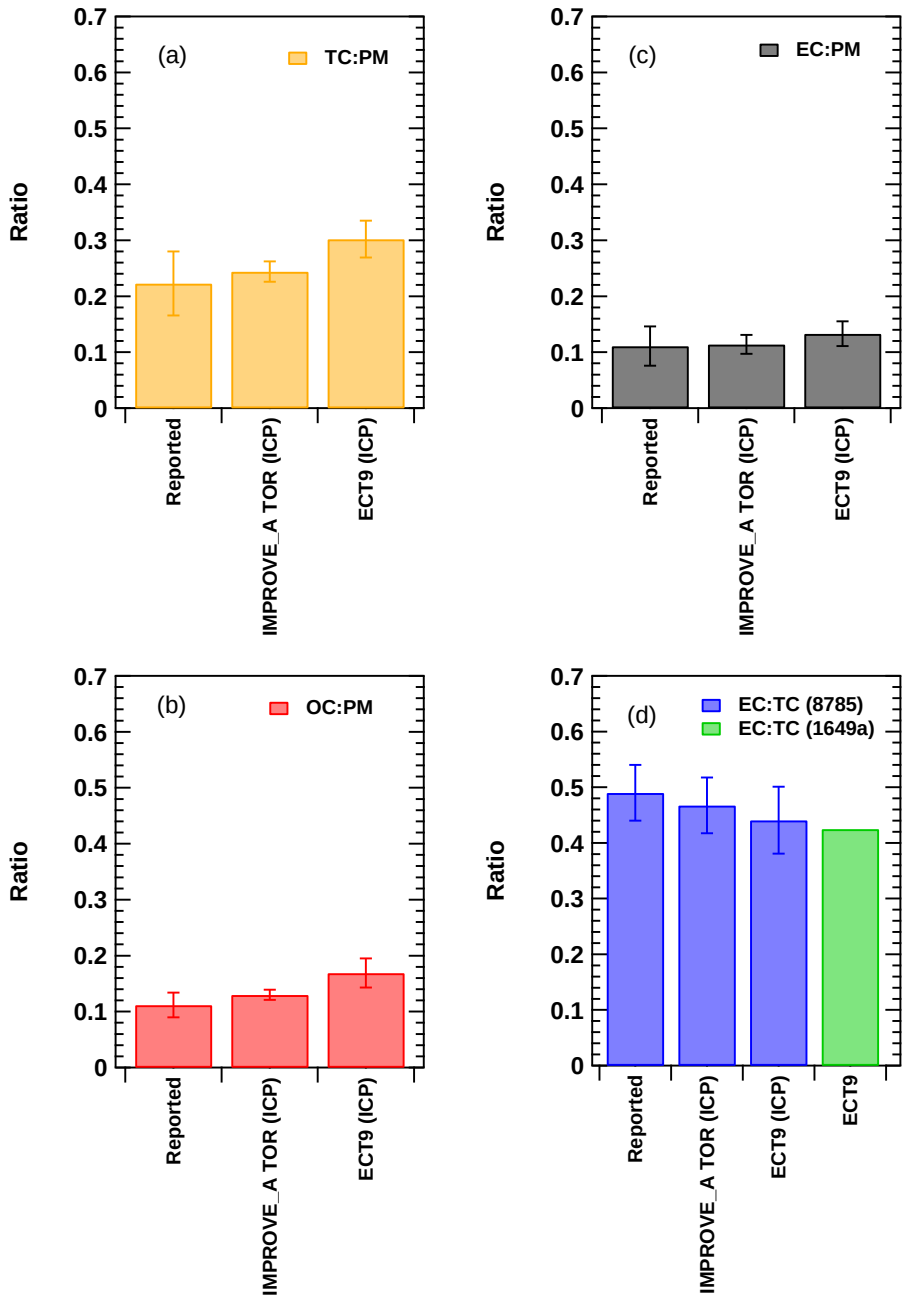

Figure 3 Comparison of: (a) TC, (b) OC, and (c) EC concentrations obtained from the same NIST SRM 8785 filters reported by ECCC following the TEA (ECT9) method and by DRI following the IMPROVE_A TOR protocol during the inter-comparison study in 2009/2010.

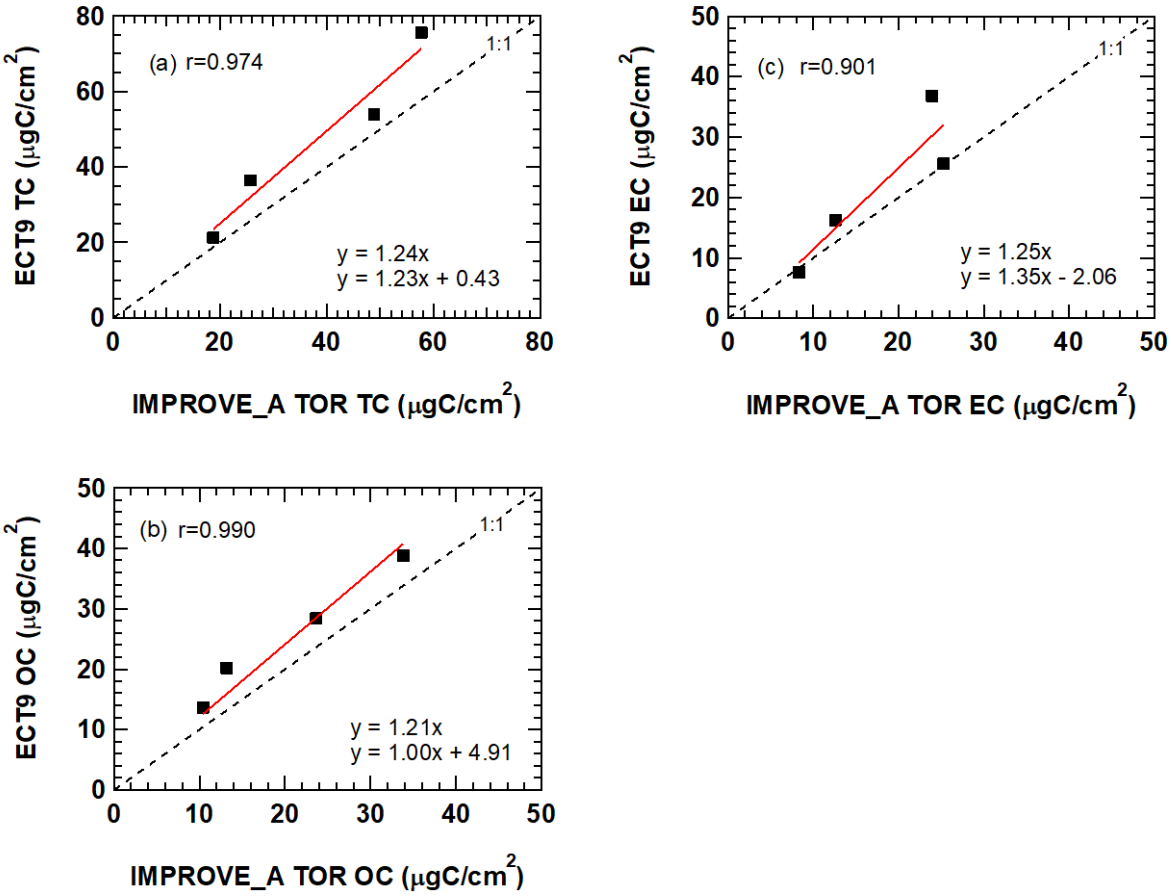

Figure 4 Monthly averaged CAPMoN (a) OC, (b) EC, and (c) POC mass concentration time series with and without vapor adsorption correction. Note that the y-axes in Figures 4b and 4c are on different scale.

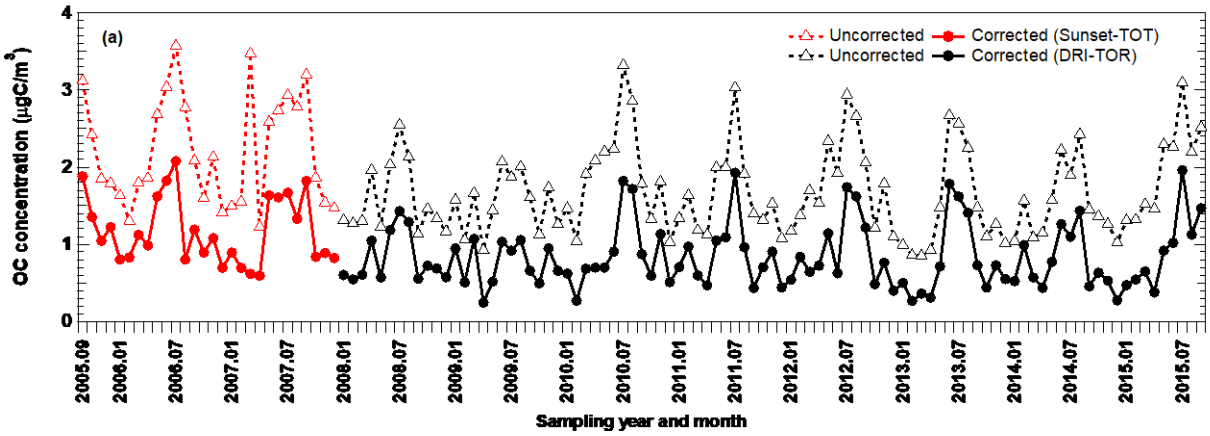

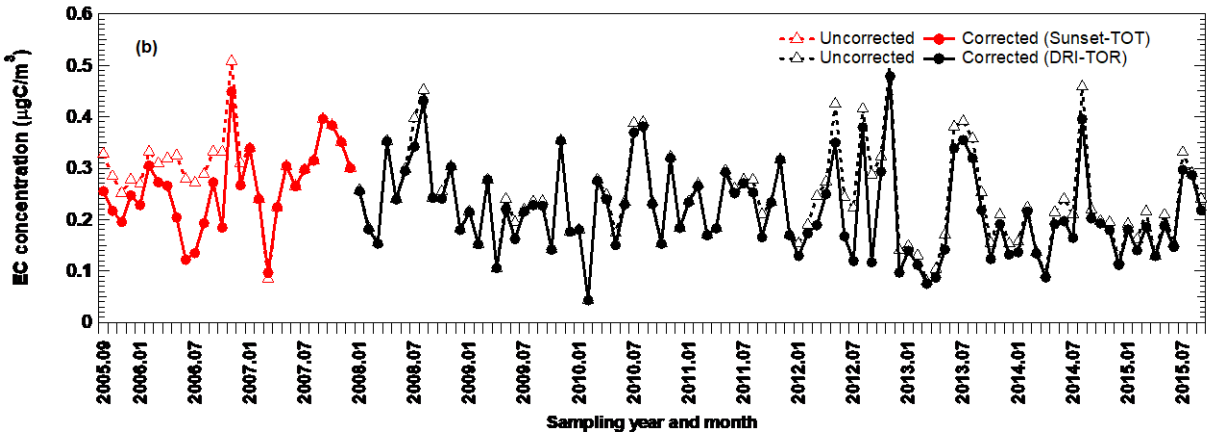

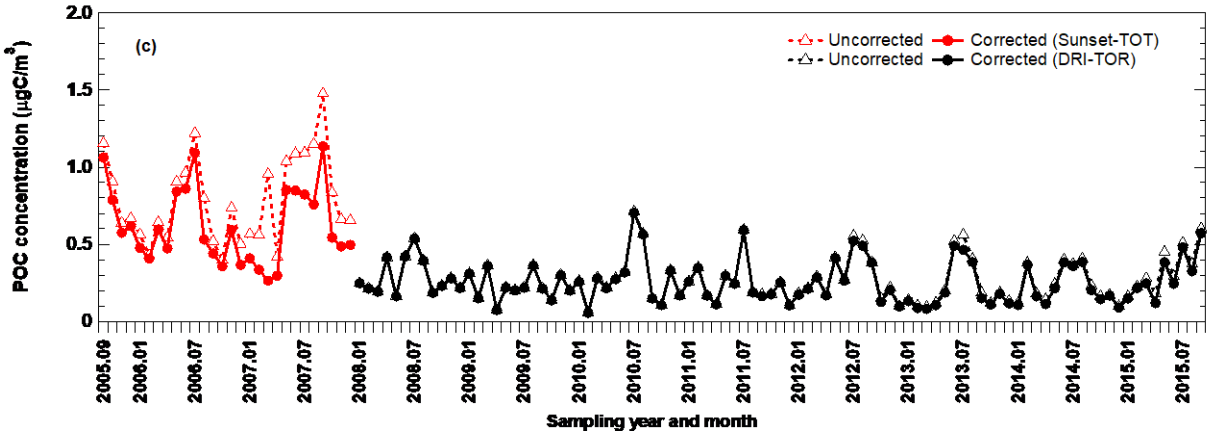

Figure 5 Relationship between the monthly averaged CAPMoN vapor adsorption corrected and uncorrected measurements for (a) TC, (b) OC, (c) EC, and (d) POC. Black solid markers represent the TOR measurements (2008-2015) analyzed by the DRI analyzer (i.e., DRI-TOR). Red open markers represent the TOT measurements before 2008 analyzed by the Sunset analyzer (i.e., Sunset-TOT). The red line represents the best-fitted linear regression of all the DRI-TOR measurements through the origin. All the corresponding statistics (i.e., best-fitted slope, correlation coefficient, total number of measurement points) are included in the legend.

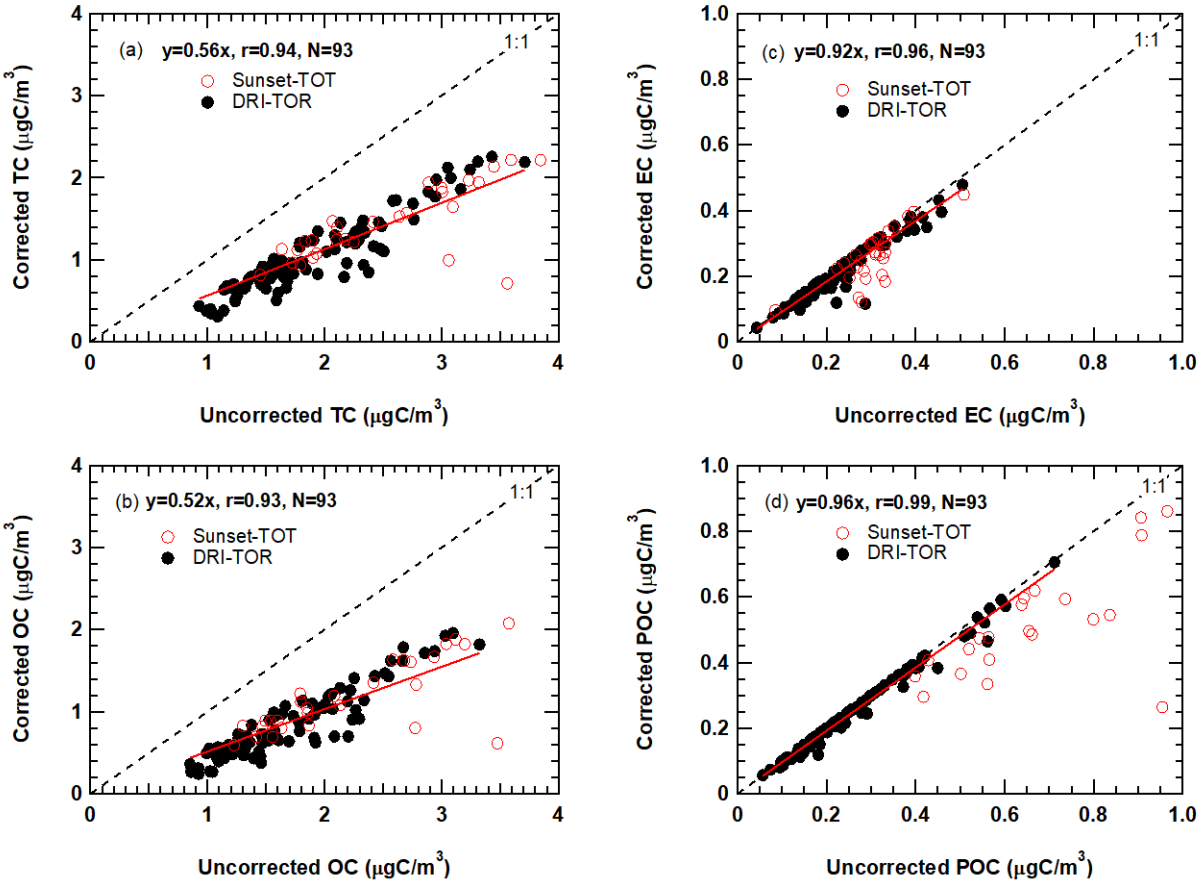

Figure 6 Monthly averaged (a) TC, (b) OC, (c) EC, and (d) POC concentration time series obtained from three different networks at Egbert. CAPMoN measurements before 2008 were obtained using Sunset-TOT method (in green) while measurements starting 2008 were obtained using DRI-TOR method (in orange).

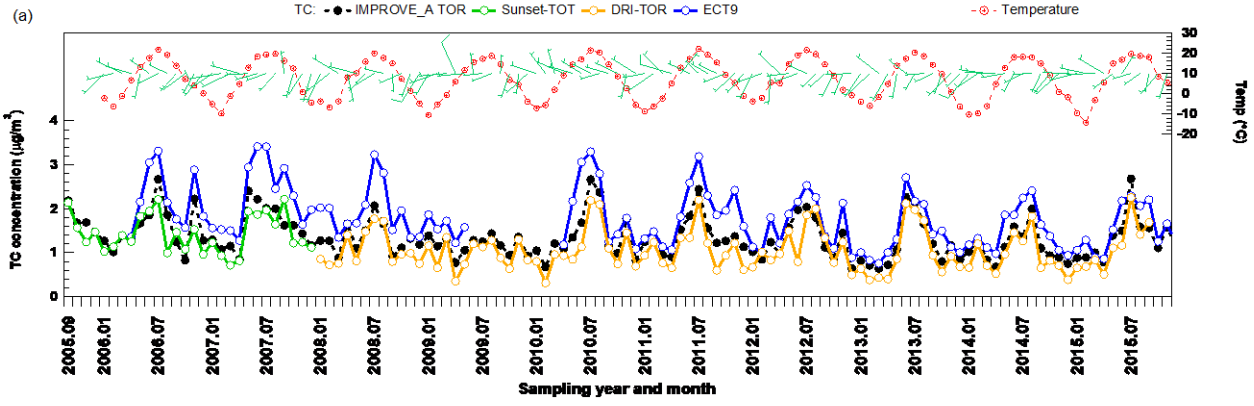

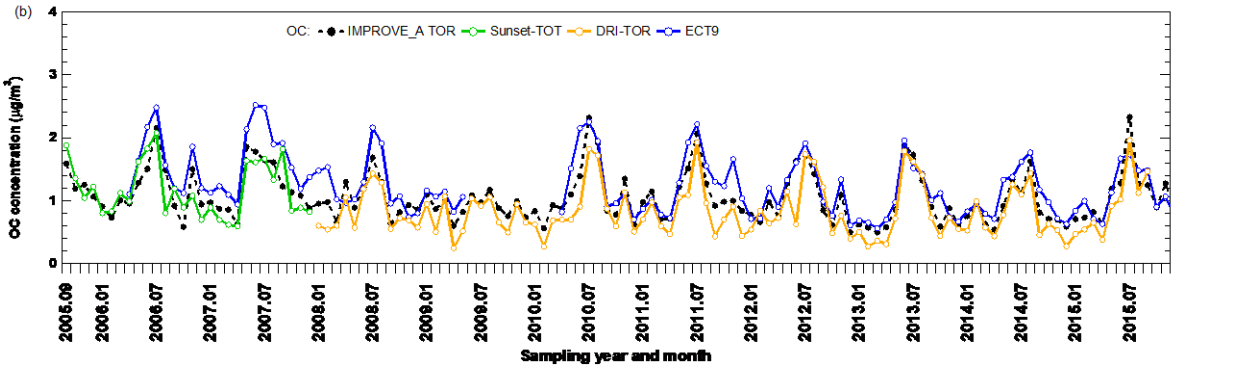

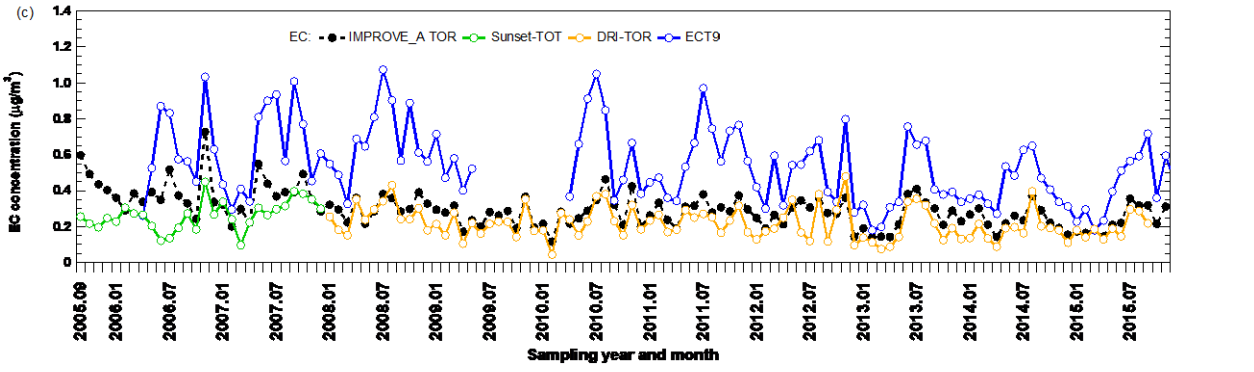

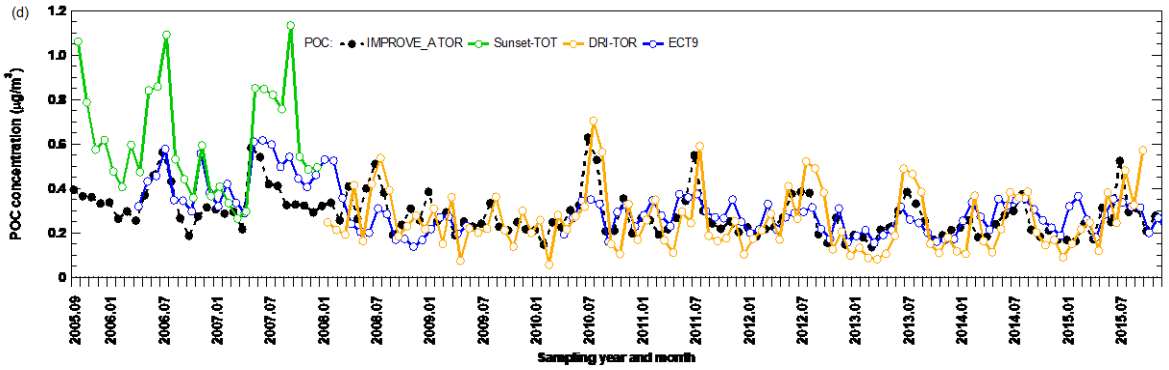

784

785

786

787 **Figure 7** Comparison of the monthly averaged carbonaceous mass concentrations from the DRI-TOR (red
788 circles and orange triangles) and ECT9 (black squares) protocols against IMPROVE_A TOR protocol. The
789 different straight lines represent the linear regression best fitted line through the origin (i.e., Regression
790 1). The fitted parameters for all corresponding data sets with (Regression 2) and without (Regression 1)
791 the y-intercept are summarized in Table 2.

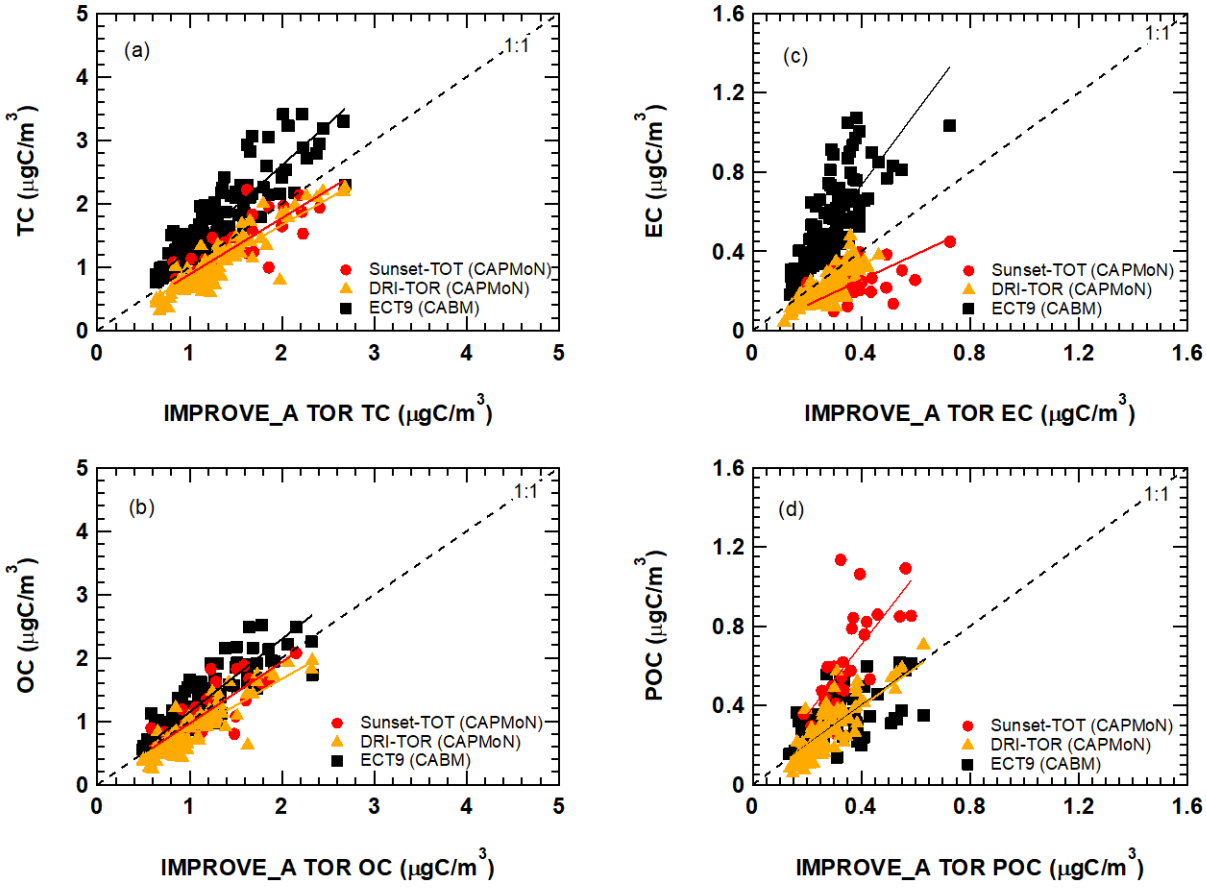

792

Figure 8 Figure shows the relationship of averaged (a) TC, (b) OC, and (c) EC concentrations from all networks as a function of ambient temperature. Each data point represent the average value of all network measurements within a 3°C temperature range. Uncertainties are standard deviations of the measurements. Red curve represents the best-fitted Sigmoid function. Figure 10(d) shows the seasonality of ECT9 POC compared to the average OC and EC seasonality. Black solid curve represents the best-fitted Sigmoid function on all ECT9 POC measurements.